Acta Crystallographica Section D
Biological Crystallography
ISSN 0907-4449

Crystallization of the crenarchaeal SRP core

Ken R. Rosendal,[a,b] Irmgard Sinning[a] and Klemens Wild[a]*

[a]Biochemie-Zentrum (BZH), University of Heidelberg, Im Neuenheimer Feld 328, D-69120 Heidelberg, Germany, and [b]EMBL, Meyerhofstrasse 1, D-69115 Heidelberg, Germany

Correspondence e-mail: klemens.wild@bzh.uni-heidelberg.de

Received 19 September 2003
Accepted 20 October 2003

Protein translocation across or targeting to membranes mediated by the signal recognition particle (SRP) is a universal mechanism conserved in all domains of life. SRP54 from the crenarchaeon *Sulfolobus solfataricus* has been recombinantly expressed and crystallized with and without SRP RNA helix 8. The RNA has been transcribed *in vitro* using ribozyme technology. Both crystal forms are perfect merohedral twins. While SRP54 alone is hemihedrally twinned, the crystals of the SRP54–helix 8 complex indicate tetartohedral twinning, which has not previously been observed in protein crystals. The tetartohedral twinning is enabled by a special diamond-like packing in a trigonal crystal.

1. Introduction

The signal recognition particle (SRP) is a ribonucleoprotein particle that targets nascent membrane and secretory proteins to the translocation machinery of the endoplasmic reticulum in eukaryotes or the plasma membrane of bacteria (Keenan *et al.*, 2001; Lutcke & Dobberstein, 1993; Walter & Johnson, 1994). SRP interacts with the ribosome, where it binds to the signal peptide of the nascent chain. The SRP–ribosome nascent-chain (RNC) complex is then targeted to the membrane-associated SRP receptor (SR) in a GTP-dependent manner (Miller *et al.*, 1993). The signal peptide is subsequently guided into the translocon, where the nascent polypeptide is translocated across or inserted into the membrane. After GTP hydrolysis in both SRP and its receptor (Miller *et al.*, 1993), the complex is resolved and SRP is prepared for a new translocation cycle. The archaeal SRP machinery represents an intermediate between the complex mammalian and the simple eubacterial systems (Zwieb & Eichler, 2002). It consists of two polypeptides (SRP19 and SRP54), an ∼310-nucleotide SRP RNA (7S RNA) and the SRP receptor protein FtsY. These components or their homologues are conserved in all domains of life. SRP54 is a three-domain protein with an N-terminal four-helix bundle, a G domain with a Ras-like GTPase fold (Freymann *et al.*, 1997) and a C-terminal M domain (methionine-rich) that is responsible for binding the signal peptide (Clemons *et al.*, 1999; Zopf *et al.*, 1990) and SRP RNA (Batey *et al.*, 2000; Romisch *et al.*, 1990). The hallmark of the SRP cycle is the binding of the signal peptide to the M domain and its release into the translocon. Both actions are regulated by the GTPase present in SRP54 and FtsY. In order to further characterize the regulation of the SRP cycle and the role of domain cross-talking in SRP54, we have crystallized SRP54 from the archaeon *Sulfolobus solfataricus* alone and in complex with its cognate binding site on SRP RNA (helix 8). The protein–RNA crystals show a complex twinning phenomenon which can be interpreted by tetartohedral merohedry.

2. Methods and results

2.1. Protein expression and purification

A gene fragment encoding amino acids 1–432 of *S. solfataricus* SRP54 was amplified by PCR using PCR primers encoding an N-terminal hexahistidine tag and a C-terminal stop codon. The fragment was cloned in the *Nco*I and *Bam*HI sites of the expression vector pET24d (Novagen). SRP54 was expressed in the *Escherichia coli* expression strain Rosetta pLyS (Novagen). The bacteria were grown in Luria–Bertani media (LB) containing kanamycin (10 mg l^{-1}) and chloramphenicol (34 mg l^{-1}) at 310 K until an optical density (OD_{600nm}) of 0.8; protein expression was then induced by addition of 1 m*M* isopropyl-1-thio-β-D-galactopyranoside (IPTG). Expression continued for 4 h at the same temperature. The harvested bacteria were resuspended in buffer *A* (50 m*M* Tris–HCl pH 8.0, 300 m*M* NaCl). Lysis was performed by sonication in the presence of Complete protease inhibitor (Roche Molecular Biochemicals) and the lysate was cleared by ultracentrifugation at 91 000*g* (average) for 60 min at 277 K (Sorvall Discovery 100, T-647.5). SRP54 was purified in a three-step procedure. The soluble fraction was enriched by nickel-affinity chromatography (Chelating Sepharose Fast Flow,

Amersham Biosciences), eluted with buffer *B* (buffer *A* containing 500 m*M* imidazole), followed by heating the pooled fractions at 343 K for 20 min. The precipitated contaminants were removed by centrifugation at 4300*g* for 10 min at 277 K (Heraeus Megafuge 1.0 R) and the supernatant was dialysed against buffer *C* (20 m*M* HEPES pH 7.5, 150 m*M* KCl, 10 m*M* $MgCl_2$). After concentrating SRP54 to about 15 mg ml^{-1} (Amicon Ultra, 30 kDa molecular-weight cutoff), the protein was applied to a gel-filtration column (Superdex 200 16/60; Amersham Biosciences). Fractions containing SRP54 were pooled and concentrated to 30 mg ml^{-1} as determined by the Bradford assay and absorbance at 280 nm.

2.2. *In vitro* transcription of SRP RNA helix 8

Helix 8 of SRP RNA was amplified by PCR using a primer containing the T7 promotor and ligated into the vector pUC18 using the restriction-enzyme sites *Kpn*I and *Xba*I. A hammerhead ribozyme in the form of an oligonucleotide adaptor molecule (Wild *et al.*, 1999) was ligated directly after the helix 8 coding region using the *Xba*I and *Hin*dIII restriction sites. After linearization with *Hin*dIII, a 47-nucleotide RNA was produced by run-off *in vitro* transcription and purified by denaturing polyacrylamide electrophoresis and electro-elution (Price *et al.*, 1995). The transcript contains 43 native nucleotides from helix 8 (nucleotides 181–223) and two non-native base pairs resulting from the T7 promoter and the ribozyme. Finally, the purified RNA was desalted in a PD10 column (Amersham Biosciences), eluted in pure water and concentrated in a Speed-Vac.

2.3. Crystallization

SRP54 and SRP54–helix 8 crystals were grown by vapour diffusion using the hanging-drop method in 24-well Linbro plates at a temperature of 291 K (Fig. 1). Crystals of SRP54 were obtained by mixing equal amounts of protein (30 mg ml^{-1}) and precipitant buffer (2–4% PEG 8000, 1–1.2 *M* Li_2SO_4). The protein–RNA crystals were produced by mixing equal amounts of SRP54–helix 8 (5 mg ml^{-1}) and precipitant buffer [acetate buffer pH 4.5, 1.26 *M* $(NH_4)_2SO_4$, 200 m*M* NaCl]. The SRP54 crystals typically grew in 1–2 d to maximum dimensions 400 × 50 × 50 µm, while the protein–RNA crystals reached their final size (50 × 50 × 30 µm) in 5–6 d.

2.4. Data collection and processing

Prior to data collection, the crystals were mounted in cryoloops (Hampton Research) and cryoprotected by transferring the crystals to either 90% mineral oil/10% Paratone-N (SRP54) or dry paraffin oil (SRP54–helix 8). The crystals were frozen by directly immersing them into liquid

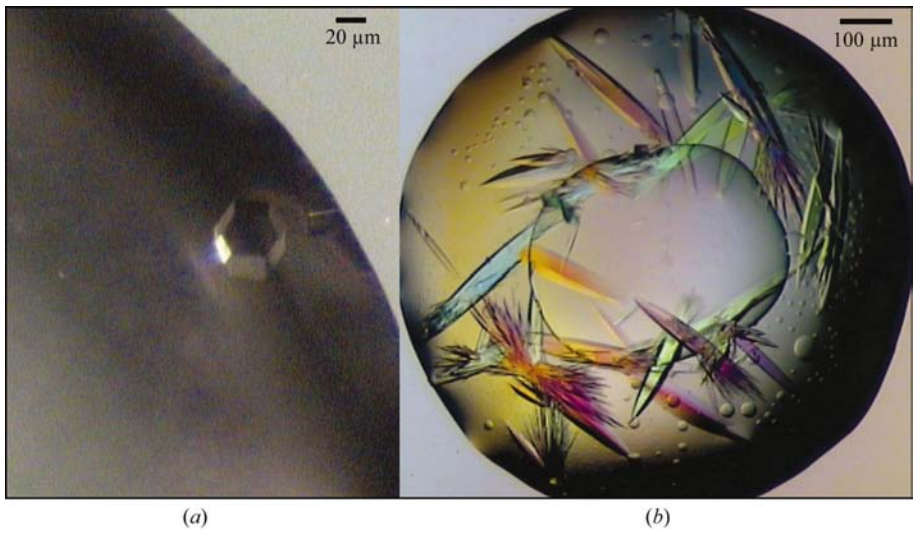

Figure 1
Crystals of SRP54 with and without SRP RNA helix 8. (*a*) Trigonal crystal of SRP54 complexed with helix 8 of SRP RNA. (*b*) Tetragonal crystals of SRP54.

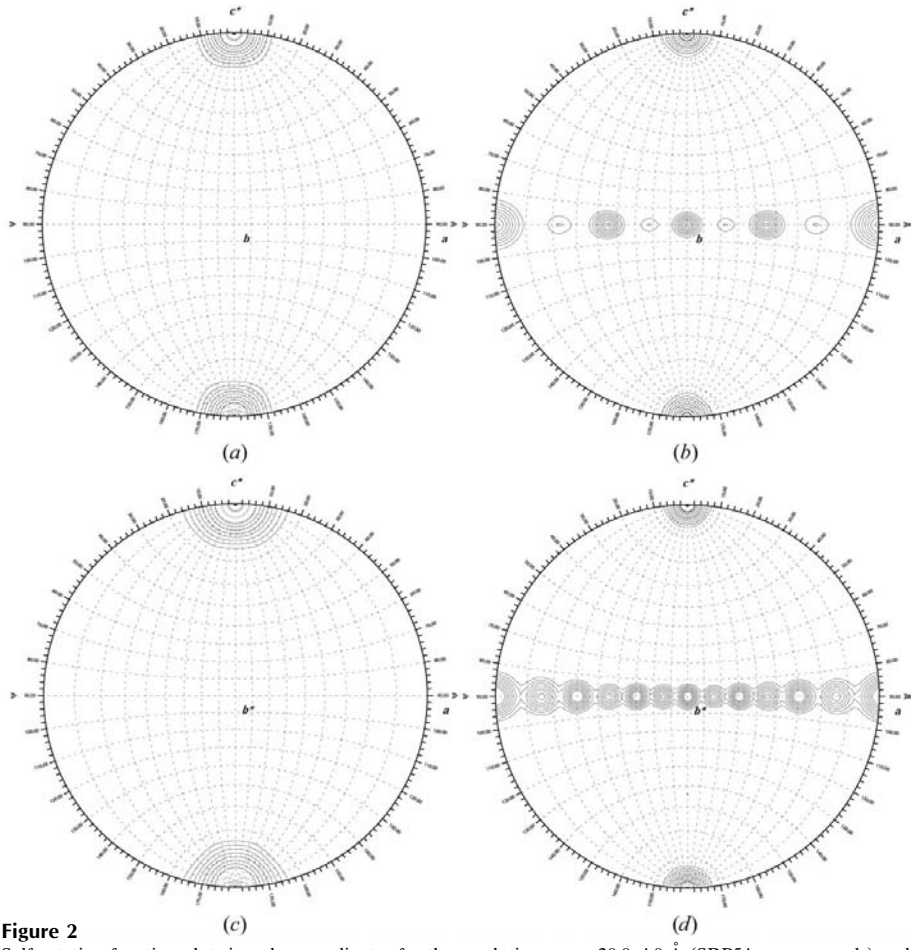

Figure 2
Self-rotation function plots in polar coordinates for the resolution range 20.0–4.0 Å (SRP54, upper panels) and 20.0–4.3 Å (SRP54–helix 8, lower panels, calculated in space groups *I*4 and $P3_1$, respectively). The following sections are shown: SRP54 (apparent point group 622), (*a*) $\kappa = 90^\circ$ and (*b*) $\kappa = 180^\circ$; SRP54–helix 8 (apparent point group 422), (*c*) $\kappa = 60^\circ$ and (*d*) $\kappa = 180^\circ$. The plots were calculated with the program *GLRF* (Tong & Rossmann, 1997). Contours start at 2σ and increase in 1.5σ intervals.

nitrogen. The data were collected at the European Synchrotron Radiation Facility (ESRF) on beamlines ID14-2 (SRP54) and ID13 (SRP54–helix 8). All data were integrated using *MOSFLM* (Leslie, 1992) and scaled, merged and truncated with the *CCP*4 package (Collaborative Computational Project, Number 4, 1994). Data statistics are listed in Table 1.

2.5. Detection of twinning

According to their apparent point-group symmetry deduced from self-rotation functions (Fig. 2), the space groups were initially determined as $I422$ (SRP54) and $P6_422$ (SRP54–helix 8; screw confirmed by molecular replacement), with one molecule per asymmetric unit in both crystal forms. Decreasing the crystal symmetries to $I4$ and $P6_4$ (or $P3_1$), respectively, did not significantly improve the data-processing statistics. The solvent contents of both crystals were rather high, with approximately 60% solvent content for SRP54 and 80% for SRP54–helix 8. Both crystal forms could be unambiguously solved by molecular replacement with either *BEAST* (Read, 2001) or *AMoRe* (Navaza & Saludjian, 1997) using the SRP54 NG domain from the closely related archaeon *Acidianus ambivalens* (PDB code 1j8m; Montoya *et al.*, 2000) as a search model. Most of the *E. coli* M domain and RNA (PDB code 1hq1; Batey *et al.*, 2000, 2001) could be placed in the resulting Fourier maps. Nevertheless, all attempts to refine the structures failed. Analysing the data sets using the twinning server (Yeates, 1997) and the *CCP*4 (Collaborative Computational Project, Number 4, 1994) and *CNS* (Brünger *et al.*, 1998) packages revealed that both data sets were highly twinned, although calculation of the twinning parameters (*i.e.* intensity statistics) was limited by the moderate resolution. The tetragonal crystals of SRP54 belong to the space group $I4$, with two molecules in the asymmetric unit. The twinning fraction was found to be about 47% and the data set could be treated as a perfect hemihedral twin.

The twinning of the SRP54–helix 8 data set was more intricate. After processing the data in all possible trigonal and hexagonal space groups and performing one step of hemihedral twin refinement in *CNS*, the space group $P3_1$ was the only one that gave a considerable drop in both the R factor (54.9 to 40.8) and $R_{\rm free}$ (54.9 to 45.6). In $P3_1$, the crystals contain four molecules in the asymmetric unit. Surprisingly, the crystals showed almost perfect twinning for all three possible twin operators ($-h$, $-k$, l; k, h, $-l$; $-k$, $-h$, $-l$), so-called tetartohedral twinning, which to our knowledge has not previously been reported in biological crystallography. Tetartohedral twinning adds extra 222 symmetry to the actual point-group symmetry of the crystal. The four molecules of the asymmetric unit are arranged in a distorted tetrahedron (to fit the trigonal crystal requirements) and the three tetrahedrons (12 molecules) of the unit cell are arranged around the 3_1 screw axis (Fig. 3). These three tetrahedrons are part of three different layers (1, 2, 3) of tetrahedrons and thus the crystal can be described as a cubic diamond-like lattice. Apart from the twinning, the orientations of the tetrahedrons in one layer are identical

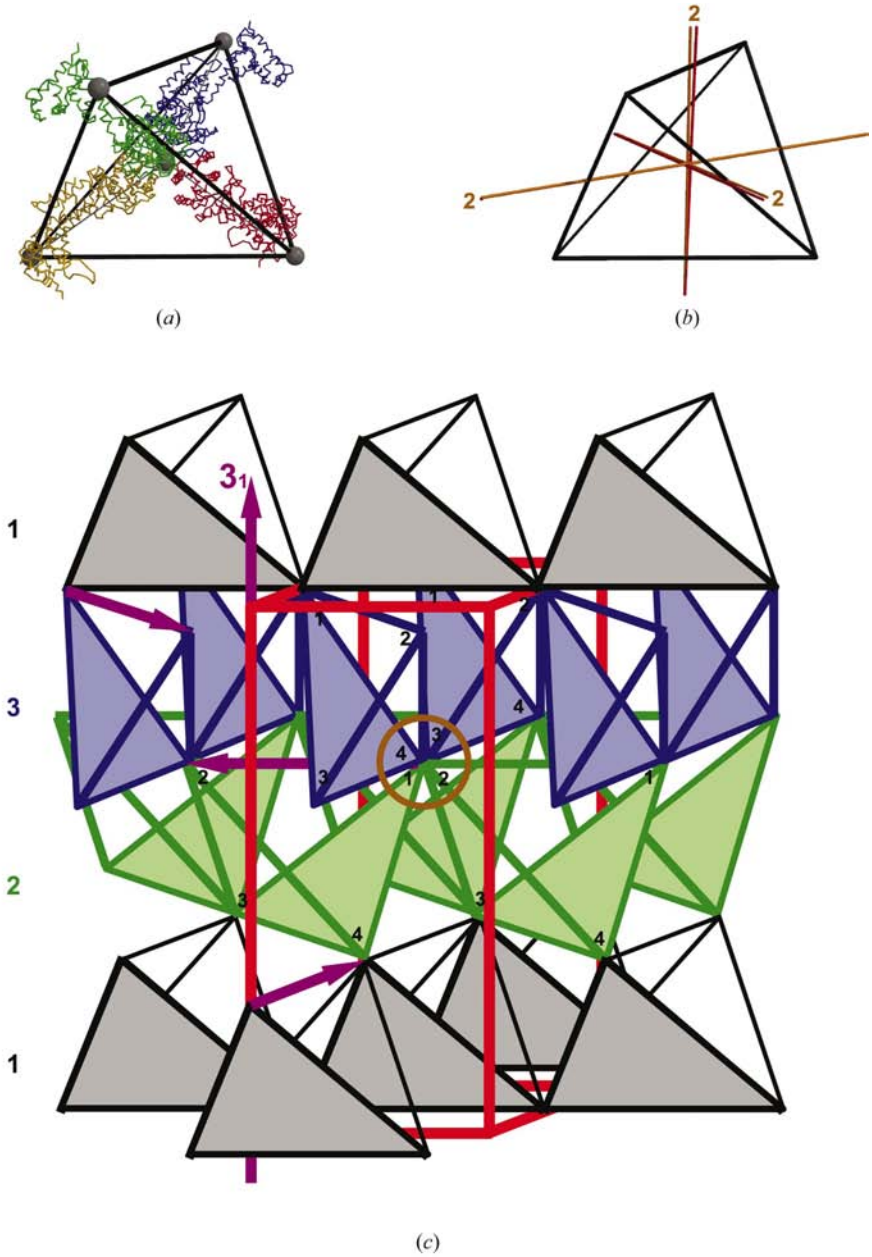

Figure 3
The diamond-like crystal packing of the SRP54–helix 8 complex. (*a*) The four molecules of the asymmetric unit are arranged in a distorted tetrahedron. The carbon positions and bonds of the superposed diamond lattice are shown in grey. (*b*) The 222 symmetry of the tetrahedron. The perfect dyads (red) cross at a single point (the central carbon) of the tetrahedron. The 222 pseudo-symmetry within the asymmetric unit is shown as orange lines. (*c*) Correlation of the unit cell with the diamond lattice. The trigonal unit cell is shown in red. The tetrahedrons forming the asymmetric unit are arranged in three layers (1, 2, 3) according to a cubic diamond lattice. The three tetrahedrons forming the unit cell are marked with a pink arrow and are arranged around the 3_1 screw axis. The four different corners are marked and would be identically arranged in one layer if the data were not twinned. The four different corners are joined together (gold circle). The tetartohedral twinning can be easily achieved by permutating the orientations of the four different corners.

Table 1
Crystallographic data.

Values in parentheses are for the highest resolution shell.

	SRP54	SRP54–helix 8
Space group	$I4$	$P3_1$
Unit-cell parameters (Å)	$a = b = 197.91$, $c = 64.31$	$a = b = 138.38$, $c = 308.59$
Wavelength (Å)	0.9740	0.9763
Resolution (Å)	40.0–4.0 (4.21–4.00)	30.0–4.1 (4.31–4.10)
Unique reflections	9576	49660
Completeness (%)	89.0 (97.9)	97.2 (98.1)
Mean $I/\sigma(I)$	4.8 (1.5)	4.0 (1.5)
Redundancy	4.2 (4.3)	1.9 (1.9)
$R_{\rm sym}$† (%)	8.3 (48.4)	8.7 (48.1)

† $R_{\rm sym} = \sum_{ij} |I_i(j) - \langle I(j)\rangle| / \sum_{ij} I_i(j)$, where $I_i(j)$ is the ith measurement of reflection j and $\langle I(j)\rangle$ is the overall weighted mean of j measurements.

and they occupy equivalent positions in all unit cells. Furthermore, the molecules can be described as 'bonds' between the C atoms of the diamond structure, with the C atoms being placed at the centre (the crystal contact of four G domains) and at the corners of the tetrahedron (the crystal contact of the NM domains). The intrinsic 222 symmetry of each tetrahedron corresponds to the non-crystallographic 222 symmetry within the asymmetric unit. The 222 symmetry is not exact (pseudosymmetry; see Fig. 3) and therefore the four corners of the tetrahedron are distinct from each other but still seem to be sufficiently similar that the tetrahedrons can be joined by either of the four different corners (apart from the twinning it is always four different corners that join; Fig. 3). This would result in four orientations of the tetrahedrons and yields the observed tetartohedral twin. Finally, it should be noted that the tetrahedral pseudosymmetrical arrangement of molecules is probably the only geometry that favours tetartohedral twinning in a protein crystal. For more complicated geometric bodies with 222 symmetry (octahedron, cube) six and eight molecules will be needed in a quasi-symmetric crystal contact and will create an even more complicated twin.

We are grateful to Ralf Moll (University of Lübeck, Germany) for genomic DNA of *S. solfataricus*. We thank Matthew Groves for stimulating discussions and suggestions on the manuscript. We also thank the ESRF staff for providing excellent support at the beamlines ID13 and ID29 at the European Synchrotron Radiation Facility (ESRF), Grenoble, France. KRR gratefully acknowledges support by the Research Council of Norway (NFR) and the EMBL PhD Programme. The work was supported by an EU Network grant (QLK-3CT) and by the DFG through the SFB-352 to IS.

References

Batey, R. T., Rambo, R. P., Lucast, L., Rha, B. & Doudna, J. A. (2000). *Science*, **287**, 1232–1239.
Batey, R. T., Sagar, M. B. & Doudna, J. A. (2001). *J. Mol. Biol.* **307**, 229–246.
Brünger, A. T., Adams, P. D., Clore, G. M., DeLano, W. L., Gros, P., Grosse-Kunstleve, R. W., Jiang, J.-S., Kuszewski, J., Nilges, M., Pannu, N. S., Read, R. J., Rice, L. M., Simonson, T. & Warren, G. L. (1998). *Acta Cryst.* D**54**, 905–921.
Clemons, W. M. Jr, Gowda, K., Black, S. D., Zwieb, C. & Ramakrishnan, V. (1999). *J. Mol. Biol.* **292**, 697–705.
Collaborative Computational Project, Number 4 (1994). *Acta Cryst.* D**50**, 760–763.
Freymann, D. M., Keenan, R. J., Stroud, R. M. & Walter, P. (1997). *Nature (London)*, **385**, 361–364.
Keenan, R. J., Freymann, D. M., Stroud, R. M. & Walter, P. (2001). *Annu. Rev. Biochem.* **70**, 755–775.
Leslie, A. G. W. (1992). *Jnt CCP4 /ESF–EAMCB Newsl. Protein Crystallogr.* **26**.
Lutcke, H. & Dobberstein, B. (1993). *Mol. Biol. Rep.* **18**, 143–147.
Miller, J. D., Wilhelm, H., Gierasch, L., Gilmore, R. & Walter, P. (1993). *Nature (London)*, **366**, 351–354.
Montoya, G., te Kaat, K., Moll, R., Schafer, G. & Sinning, I. (2000). *Structure Fold. Des.* **8**, 515–525.
Navaza, J. & Saludjian, P. (1997). *Methods Enzymol.* **276**, 581–594.
Price, S. R., Ito, N., Oubridge, C., Avis, J. M. & Nagai, K. (1995). *J. Mol. Biol.* **249**, 398–408.
Read, R. J. (2001). *Acta Cryst.* D**57**, 1373–1382.
Romisch, K., Webb, J., Lingelbach, K., Gausepohl, H. & Dobberstein, B. (1990). *J. Cell Biol.* **111**, 1793–1802.
Tong, L. & Rossmann, M. G. (1997). *Methods Enzymol.* **276**, 594–611.
Walter, P. & Johnson, A. E. (1994). *Annu. Rev. Cell Biol.* **10**, 87–119.
Wild, K., Weichenrieder, O., Leonard, G. A. & Cusack, S. (1999). *Structure Fold. Des.* **7**, 1345–1352.
Yeates, T. O. (1997). *Methods Enzymol.* **276**, 344–358.
Zopf, D., Bernstein, H. D., Johnson, A. E. & Walter, P. (1990). *EMBO J.* **9**, 4511–4517.
Zwieb, C. & Eichler, J. (2002). *Archaea*, **1**, 27–34.